



Research Article

Optimizing seismic performance: Integrating friction dampers into spherical liquid tanks

Yunus UÇAR^{*1}, Mehmet Fatih ALTAN²

¹Department of Civil Engineering, İstanbul Aydın University, İstanbul, Türkiye

²Department of Civil Engineering, İstanbul Arel University, İstanbul, Türkiye

ARTICLE INFO

Article history

Received: 28 March 2024

Revised: 10 May 2024

Accepted: 02 July 2024

Key words:

Earthquake resilience, friction dampers, LNG tank, retrofit, seismic performance, sloshing effect

ABSTRACT

This study addresses the vital challenge of ensuring the safe storage of Liquid Natural Gas (LNG) in spherical tanks during seismic events, focusing on the crucial balance between meeting seismic performance criteria and mitigating economic losses due to potential operational disruptions from necessary retrofitting efforts. In response to this challenge, we present a case study on retrofitting an LNG tank near the North Anatolian Fault (NAF) line of Türkiye. Through a comprehensive seismic evaluation, this study reveals inadequacies in the existing case's compliance with seismic criteria. It suggests a remedy involving the increased stiffness of lateral force-resisting members coupled with the utilization of friction dampers. Following the proposed stiffness increase achieved through retrofitting, our approach is fundamental to exploring alternative damping mechanisms designed to enhance the steel column-brace support structure. One of the key design challenges is the unique dynamic behavior of LNG, especially its sloshing during earthquakes, which necessitates a comprehensive understanding of fluid-structure interaction for accurate modeling and analysis. Through a series of transient analyses incorporating actions, we evaluate the effectiveness of the proposed retrofitting measures on the structure. Our findings introduce a feasible and efficient retrofitting strategy, marked by minimal operational interruption, primarily by avoiding the extensive demolition and reconstruction typically required.

Cite this article as: Uçar, Y., & Altan, M. F. (2024). Optimizing seismic performance: Integrating friction dampers into spherical liquid tanks. *J Sustain Const Mater Technol*, 9(3), 294–304.

1. INTRODUCTION

As lifeline structures of strategic importance, liquid storage tanks are extensively used in the petroleum industry, urban water resources management, and nuclear power facilities [1]. During an earthquake, LNG storage tanks may experience significant gas pressure, potentially causing damage and permanent deformation to the steel structure [2]. Damage to liquid storage tanks can disrupt essential infrastructure and may result in fires or environmental pollution due to leaks of flammable substances or hazardous chemicals [1]. These tanks must comply with high seismic performance standards,

given the risk of explosions or fires from LNG leaks. Therefore, conducting an extensive seismic assessment of these tanks is essential. If an LNG tank fails to satisfy the required seismic performance criteria, retrofitting with either conventional or advanced solutions becomes necessary. However, the prolonged downtime and disruption in confined spaces often render traditional retrofitting methods impractical. Additionally, seismic forces tend to increase as the structure's stiffness increases, necessitating foundation expansions [3]. Therefore, exploring alternative solutions to introduce additional damping to these structures is sensible, aiming to limit seismic drifts without significantly increasing stiffness.

*Corresponding author.

E-mail address: yunusucar@stu.aydin.edu.tr, yucar@ipkb.gov.tr



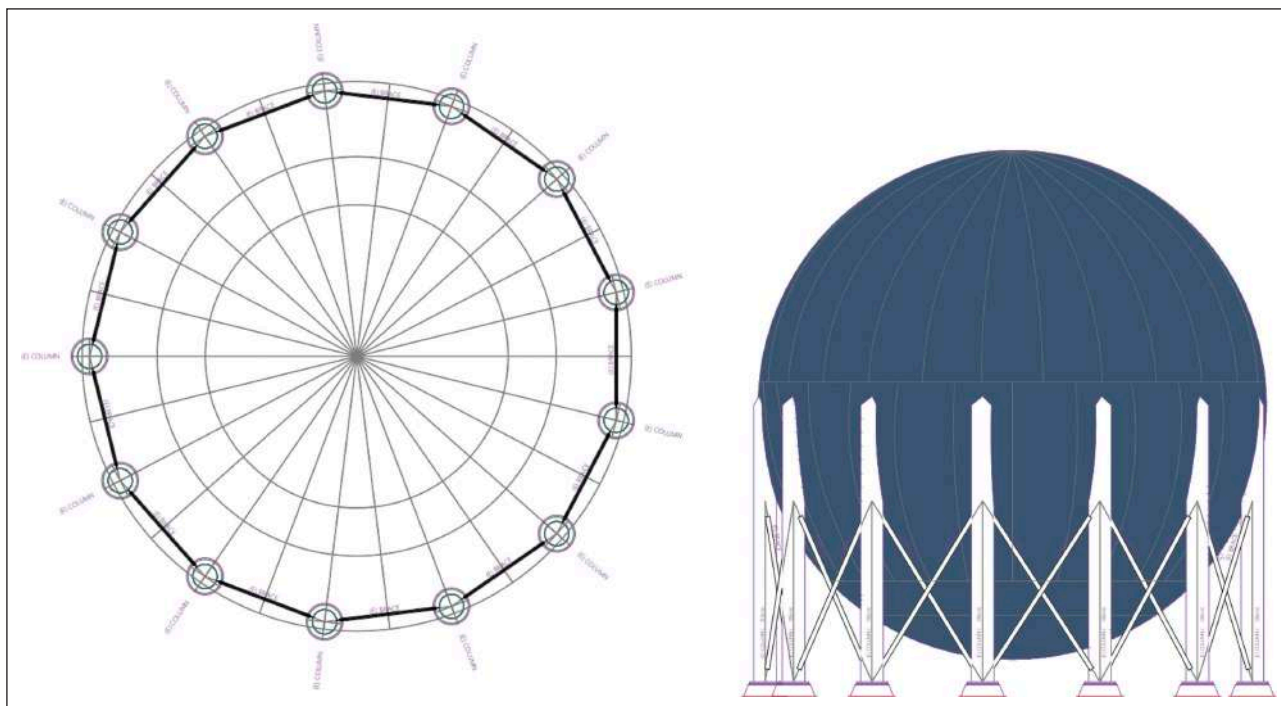


Figure 1. Plan and elevation view of the LNG tank.

Previous studies have investigated the seismic performance of LNG tank structures using seismic energy-dissipating devices such as seismic isolators and dampers. Seismic isolators, positioned at the base to isolate the superstructure from earthquakes, exhibit low horizontal stiffness but substantial vertical stiffness and strength to support structural weight without differential movement. While isolators significantly reduce acceleration, their horizontal flexibility increases horizontal displacements [1]. Gregoriou et al. [4] conducted dynamic analyses of LNG tanks with seismic isolators, resulting in considerable reductions in base shear and maximum strains. Jadhav et al. [5] explored the impact of different isolator settings on the seismic response of base-isolated fluid storage tanks. However, structures located in near-fault areas may experience increased displacement demands due to large-pulse ground motions [6]. Saha et al. [7] investigated the seismic behavior of liquid storage tanks equipped with sliding systems and elastomer bearings near fault lines. Based on the findings of the study by Çerçevik et al. [8], it can be inferred that base-isolated structures in near-fault locations may require additional damping devices such as viscous or friction dampers. Structural dampers with passive control systems operate through various mechanisms, including metallic, friction-based, viscous, and viscoelastic. In Çalım et al. [9] and Güllü et al. [10], the advantages and disadvantages of various structural dampers with passive control systems are discussed. Notably, friction dampers are commonly favored due to their affordability, effectiveness, and compatibility with multiple bracing types [11]. Furthermore, the stability and rigidity offered by friction dampers make them particularly appealing [12].

The sloshing effect has also been a focal point in prior research. Housner [13] used two lumped mass models for storage tanks, assuming complete rigidity of the tank walls and ideal liquid dynamics. Haroun and Housner [14] introduced a simplified mechanical model that considers both the liquid-solid interaction and the elastic deformation of the tank walls when subjected to stress. This approach to modeling LNG storage tanks incorporates various assumptions and simplifications to navigate the complexities of fluid-structure interaction.

In this case study, we assessed the seismic performance of an existing steel LNG tank, considering the fluid-structure interaction and proposing retrofitting measures that include the utilization of friction dampers. The study is organized into several sections: Part 2 is an overview of the existing structure, including structural details, soil conditions, and regional seismicity. Part 3 focuses on the methodology for modeling and analysis. The seismic assessment process and retrofitting design are discussed in Parts 4 and 5, respectively. Finally, our concluding remarks are summarized in Part 6.

2. MATERIALS AND METHODS

2.1. Existing Structure

This section presents an overview of the spherical LNG tank's structural properties, corresponding site conditions, and regional seismicity.

2.1.1. Structural Details

Considering that the LNG tank in question was designed in 1990 and is located in a region of high seismic activity, it has become necessary to evaluate the structure against current performance-based design codes and specifications. The plan and elevation view of the structure are depicted in Figure 1.

Table 1. Structural member properties

Diameter of LNG Tank	21.2 m
Column section	CHS1000/10.1
Column height	12.1 m
Spherical tank wall thickness	Varies
Brace section	205x43 mm

Table 2. Site condition parameters

Shear Wave Velocity (average) (V_{s30})	400–450 m/s
Soil Class (ASCE7-16)	C
Allowable Soil Bearing (σ_{all})	200 kPa
Vertical Subgrade Modulus (K_v)	75000 kN/m ³
Horizontal Subgrade Modulus (K_H)	35000 kN/m ³
Average Shear Strength of Soil (S)	140 kPa
Ground Water Level	–

Thirteen steel columns support the tank, and steel braces are utilized as lateral load-resisting members. Table 1 provides a summary of structural member properties.

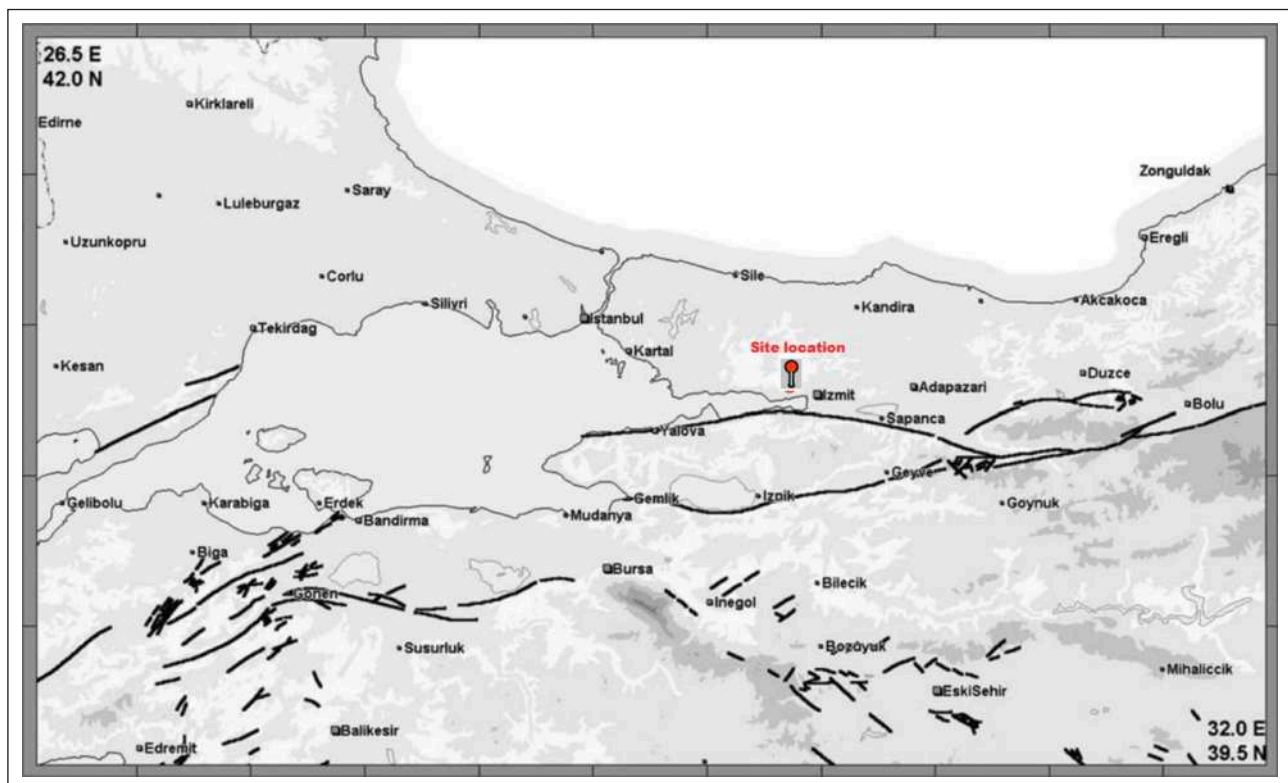
2.1.2. Site Conditions

The LNG Tank is located on a site featuring a 1-meter-thick layer of fill soil. Beneath this layer lies clayey sand soil mixed with gravel at specific points. There were no indications of groundwater presence throughout six boring operations conducted on the site. The parameters detailing the site conditions are summarized in Table 2.

2.1.3. Seismicity

The exact location of the site is marked in red in Figure 2. Regarding regional seismicity, the LNG tank is in the Marmara region of Türkiye, a region rich in history as the cradle of numerous civilizations and the epicenter of several destructive earthquakes [15]. The area's seismotectonic characteristics, fault segments, and the related seismic source parameters have been the research focus for many years, accompanied by earthquake catalogs covering historical and instrumental periods. As a result, various studies have been conducted to analyze the seismic sources of this region. In our research, source parameters were adopted from Erdik et al. [15], and the SHARE project model [16] was also employed. While deterministic and probabilistic seismic hazard analyses were carried out for the site, they are not detailed in this study as they fall outside its scope. Still, we provide the peak ground acceleration (PGA=0.96g) and the spectral values ($S_s=2.41g$ and $S_1=1.24g$) obtained for the considered event (with a 2% probability of exceedance in 2475 years).

The site is within 15 km of an active fault, necessitating the consideration of near-fault effects. For this purpose, CALTRANS (2013) near-fault model [17] has been employed in this study (Fig. 3). By deriving site-specific acceleration values and near-fault amplification factors, we constructed the simplified target design spectrum curve by ASCE 7–10 [18]. Figure 4 demonstrates the MCER spectrum, which aligns with the DD-1 design level for the Turkish Seismic Code (TSC) (2018) [19].

**Figure 2.** Site location illustrated on the active fault map of the region [15].

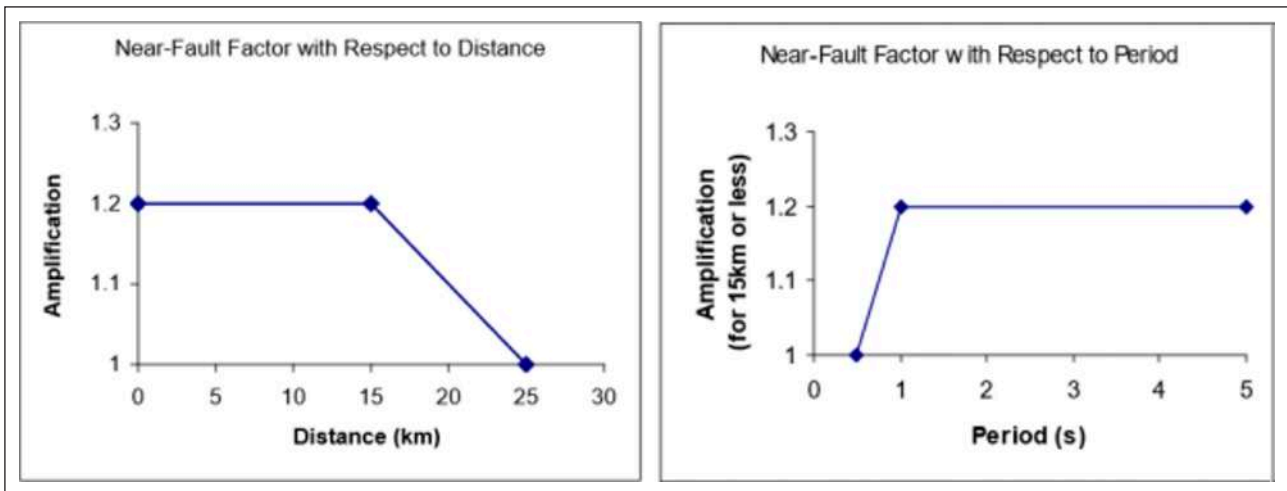


Figure 3. Near-fault effect by CALTRANS (2013) [15].

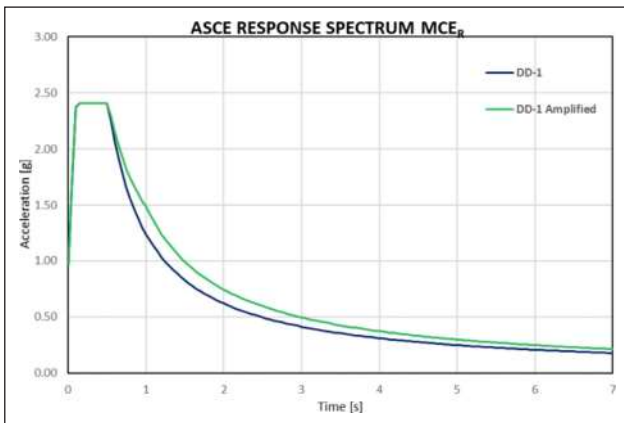


Figure 4. Simplified design spectrum.

2.2. Structural Modelling and Analysis

Analyses of the structural behavior of the LNG storage tank under seismic loads were conducted utilizing the fluid-structure interaction (FSI) approach, which integrates finite element analysis (FEA) and computational fluid dynamics (CFD) models within ANSYS.

2.2.1. Analysis Model of the Existing Structure

The development of the structural analysis model commenced with specifying the sheet thicknesses for the shell elements. These thicknesses, applied across the entire structure, are depicted visually in Figure 5. A minimum sheet thickness of 5mm was applied to the lamellae in the 13 steel columns, while the base plates featured the thickest sheet metal, with a wall thickness of 51mm, as shown in Figure 5.

The mesh necessary for the finite element analysis was generated using linear SHELL181 elements for the sheet metal components. The model comprises 65,000 nodes and 55,000 elements. Connections across all components are established through contact elements, with sourced connections defined as edge-to-edge or edge-to-surface types, depending on the requirements. The contact elements employed include CONTA172, CONTA175, and TARGE170.

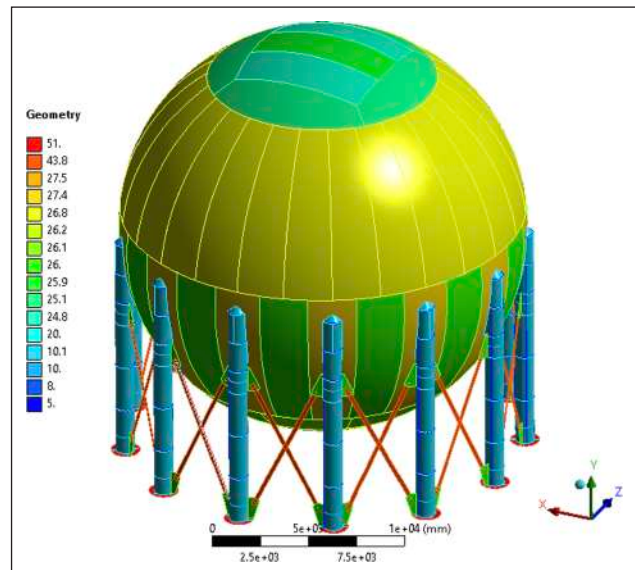


Figure 5. FEA model of the tank-sheet thickness- isometric view.

The adequacy of the mesh's resolution was confirmed through natural frequency analyses conducted on an empty tank, ensuring the mesh's reliability for the study. A mesh convergence study was undertaken using three distinct mesh sizes: 600 mm, 300 mm, and 150 mm, as depicted in Figure 6. The study's findings determined that the optimal mesh size for the main shell components is 300 mm, while 150 mm is suitable for the other parts. The final configuration of the meshed model is demonstrated in Figure 7.

2.2.2. LNG Mass Modeling and Fluid-Structure Interaction: Simulating Hydrostatic Pressure and LNG Mass

The fluid-structure interaction (FSI) method allows for accurate simulations of structural and fluid components. This approach effectively models the hydrostatic pressure induced by LNG and its mass inertia and dynamic behavior with high precision and without numerical issues. Due to the requirement for iterative data exchange between the

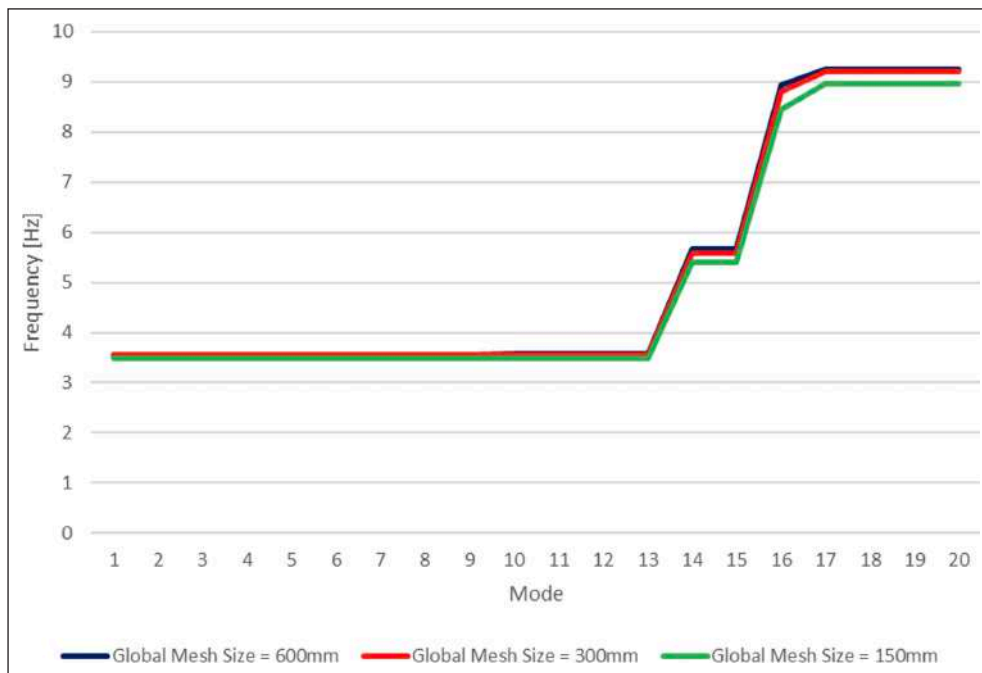


Figure 6. Mesh convergence analysis- comparison of natural frequencies of an empty tank.

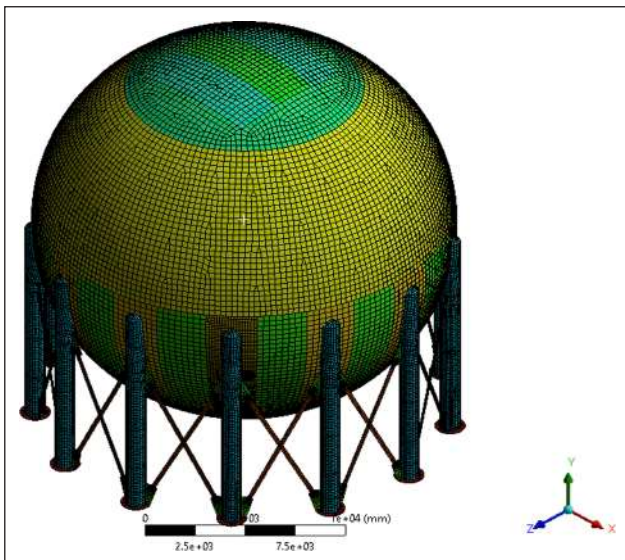


Figure 7. Analysis model with meshes for structural analysis- isometric view.

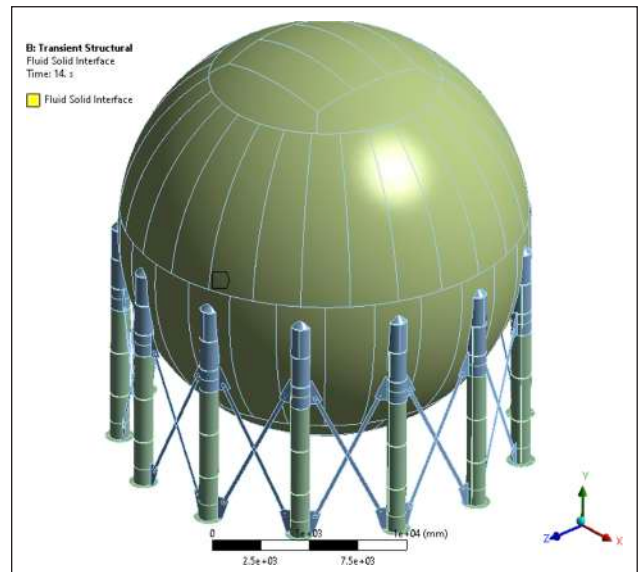


Figure 8. Pressure deformation definition for FSI analysis.

structural and fluid model solvers, this type of analysis tends to have relatively longer resolution times.

In the finite element analysis model, movement in all translational directions is restricted to zero at the joint points on the 13 baseplate surfaces.

Standard gravity acceleration, directed vertically in the Y-axis, is applied as 9.8066m/s^2 for the entire structure.

The pressure load data, derived from the CFD solution, is assigned for the shell surfaces. In solving the FSI problem, the deformations occurring on these surfaces are relayed to the CFD solver. Subsequently, both hydrostatic and dynamic pressure values calculated by the CFD solver are transferred back to these surfaces as a pressure load, as illustrated in Figure 8.

The CFD model was developed with a mesh featuring an element size of 300 mm to accommodate various solvers. This mesh comprises 220,000 elements, as illustrated in Figure 9. The model configures the interface between LNG and air for the volume-of-fluid (VOF) method. The liquid level within the tank is determined using the software's volumetric ratio functions. By employing the values of 366,400 kg for the empty weight and 3,216,400 kg for the operating weight, the volume of LNG was calculated to be 4913.79 m^3 . The specific Gravity of LNG is taken as 580 kg/m^3 .

The model characterizes LNG and air as two distinct immiscible fluids through the multi-phase analysis method. The Volume of Fluid (VOF) method determines the

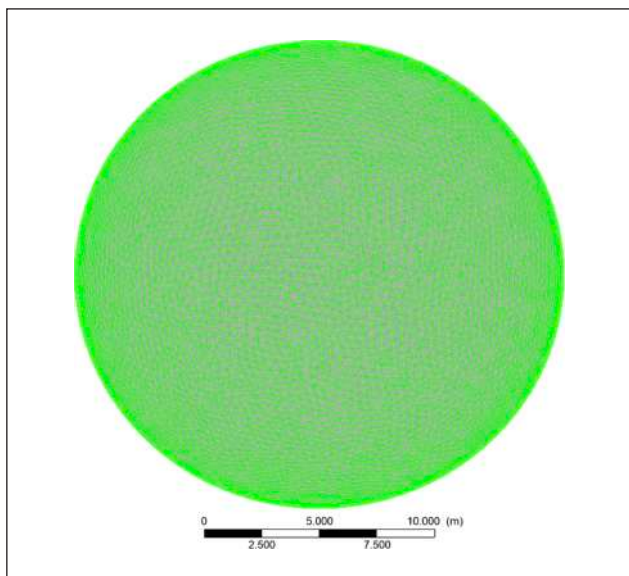


Figure 9. Mesh size for CFD analysis – 300 mm element size with 220,000 elements.

fluid interface. At each iteration of the solution, hydrostatic and dynamic pressures derived from the CFD model are transferred to the structural model (Fig. 10). The material properties considered in the analysis of these fluids are detailed in Table 3.

The model's accuracy was verified by comparing the reaction force values derived from static analysis. The total reaction force was anticipated to be 31.54MN, and the study yielded a result of 31.50MN. This indicates a mere 0.23% discrepancy between the numerical model and the engineer's calculations, demonstrating a high level of agreement.

2.3. Seismic Assessment

The objective is to achieve the Life Safety (LS) performance level under the Maximum Considered Earthquake (MCE_R) conditions.

To assess the structure's seismic performance, 11 pairs of earthquake ground motions presented in Table 4 were selected and scaled to align with the target spectrum for an

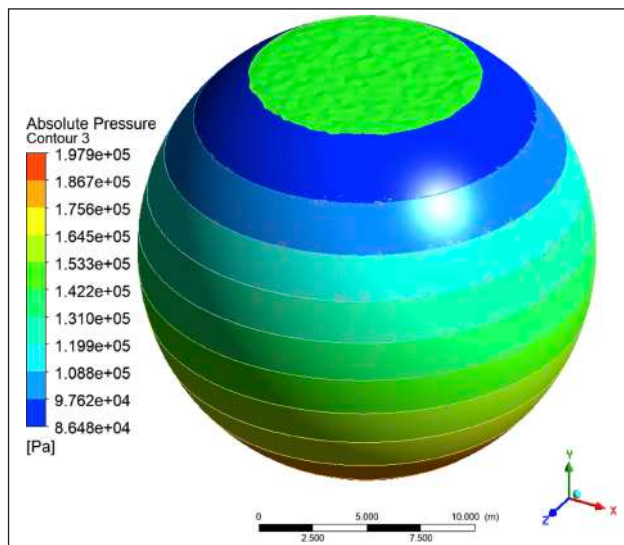


Figure 10. Free LNG surface (green color) and hydrostatic pressure distribution.

Table 3. Material properties of fluids

Material	Specific gravity (kg/m ³)	Viscosity (kg/ms)
LNG	580	0.00113
Air	1.185	1.831e-5

earthquake level corresponding to a return period of 2475 years (2% probability of exceedance in 50 years). Another Yarımca record from the Kocaeli Earthquake has also been used in the retrofitted case analysis to examine the structure's response to pulse actions.

Although recent studies have shown that energy spectra should be used for earthquake record scaling, simple scaling was used in this study [20]. Studies have also shown that the site-dominant period is an essential criterion for scaling [21, 22].

The scaling process involved adjusting both components of the seismic records to RotD100, as the most critical impact on such structures often results from maximum ground motion in a single direction. A com-

Table 4. Selected ground motion records for time history analysis

Record name	Earthquake name	Magnitude	Joyner-Boore distance (km)	Vs30 (m/s)	Style of faulting
RSN6	Imperial Valley-02	6.95	6.09	213.44	Strike-slip
RSN26	Hollister-01	5.6	19.55	198.77	Strike-slip
RSN30	Parkfield	6.19	9.58	289.56	Strike slip
RSN95	Managua, Nicaragua-01	6.24	3.51	288.77	Strike-slip
RSN99	Hollister-03	5.14	8.85	198.77	Strike-slip
RSN102	Northern Calif-07	5.2	8.2	219.31	Strike-slip
RSN147	Coyote Lake	5.74	8.47	270.84	Strike-slip
RSN158	Imperial Valley-06	6.53	0.0	259.86	Strike-slip
RSN214	Livermore-01	5.8	15.19	377.51	Strike slip
RSN233	Mammoth Lakes-02	5.69	2.91	382.12	Strike slip
RSN236	Mammoth Lakes-03	5.91	2.67	382.12	Strike slip

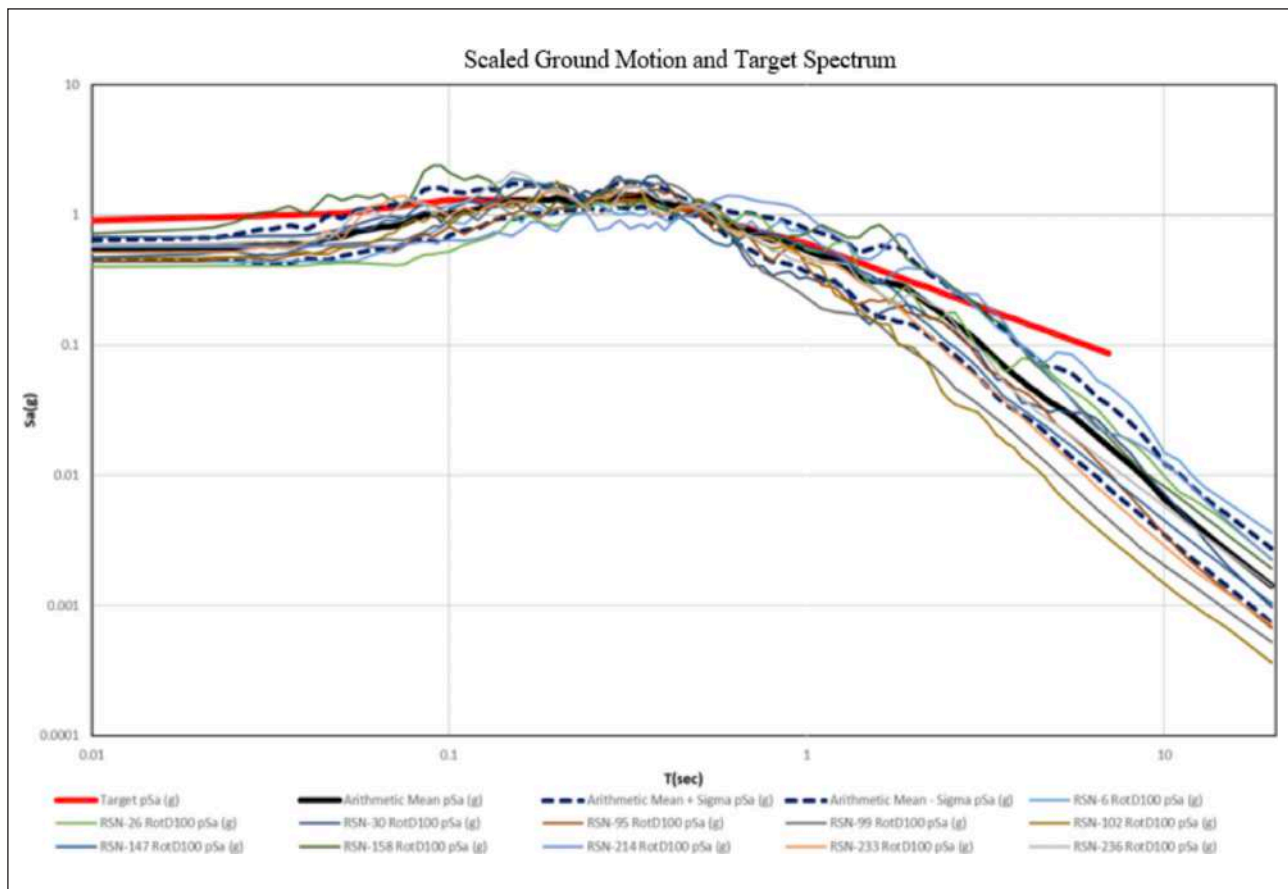


Figure 11. Scaled ground motions vs. specific target response spectrum (semi-log scale).

Table 5. Analysis results for friction dampers with different yield strengths and base shear reduction

	Existing	Yield strength [kN]				
		100	200	350	500	1000
Base Shear [kN]	27359.73	8711.09	8777.27	8623.73	8918.18	11286.09
Top Column Displacement [cm]	12.55	17.98	14.42	12.41	11.16	8.37
P [kN]	4799.91	3043.55	3204.27	3184.73	3234.36	3543.73
M2 [kNm]	1297.91	2127.55	1546.64	1796.45	1643.09	1313.73
M3 [kNm]	2441.55	2997.91	3225.82	2303.55	1986.91	1679.18
Link Displacement [cm]	–	5.51	4.05	3.26	2.75	1.60

parison between the target spectrum and the spectra of scaled ground motions is displayed in Figure 11, utilizing a semi-logarithmic scale.

During seismic performance assessment, steel columns and brace elements have been checked against criteria provided in ASCE41. Accordingly, the columns' total rotation and brace axial deformations have been calculated. The shell stresses have also been monitored. Key results from the seismic performance assessment include the columns' rotation and braces' axial deformation, as shown in Figure 12. Finally, the maximum top displacement values were calculated for each ground motion. The top displacement values and the seismic-induced deformation of the LNG tank are also visualized in Figure 13.

After assessing the existing structure, it was determined that it failed to meet the necessary criteria, indicating a need for retrofitting. The failing mechanism starts with compression failure and subsequent buckling of the brace elements, followed by the exceedance of the plastic rotation capacity of the column elements.

2.4. Seismic Retrofit Design

Various retrofit options have been researched, including (A) conventional retrofitting using larger columns and brace sections, (B) seismic isolation, (C) viscous dampers, and (D) friction dampers. Conventional retrofit alternatives have been eliminated due to the extended construction downtime and foundation retrofit requirement, which prevent access to critical nearby facilities.

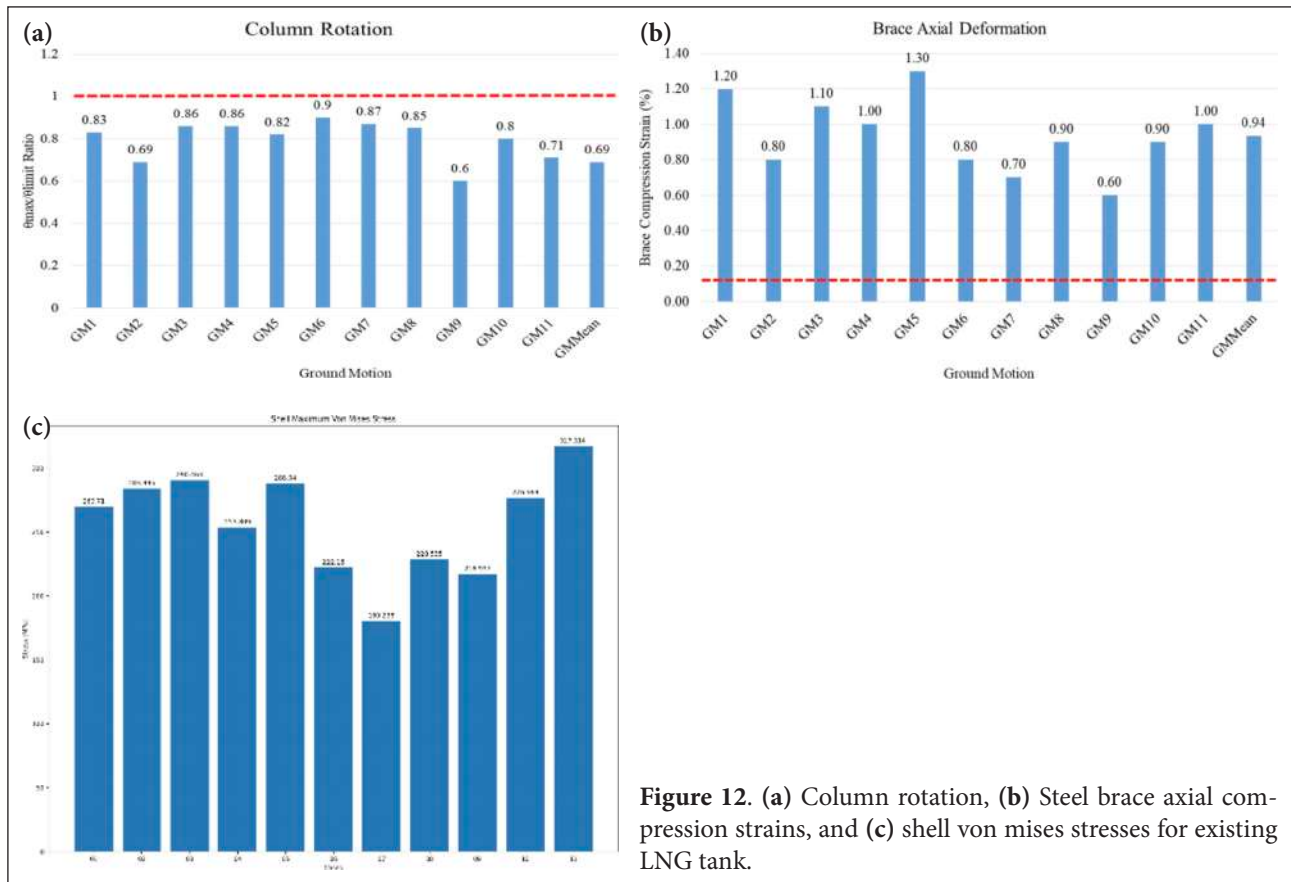


Figure 12. (a) Column rotation, (b) Steel brace axial compression strains, and (c) shell von mises stresses for existing LNG tank.

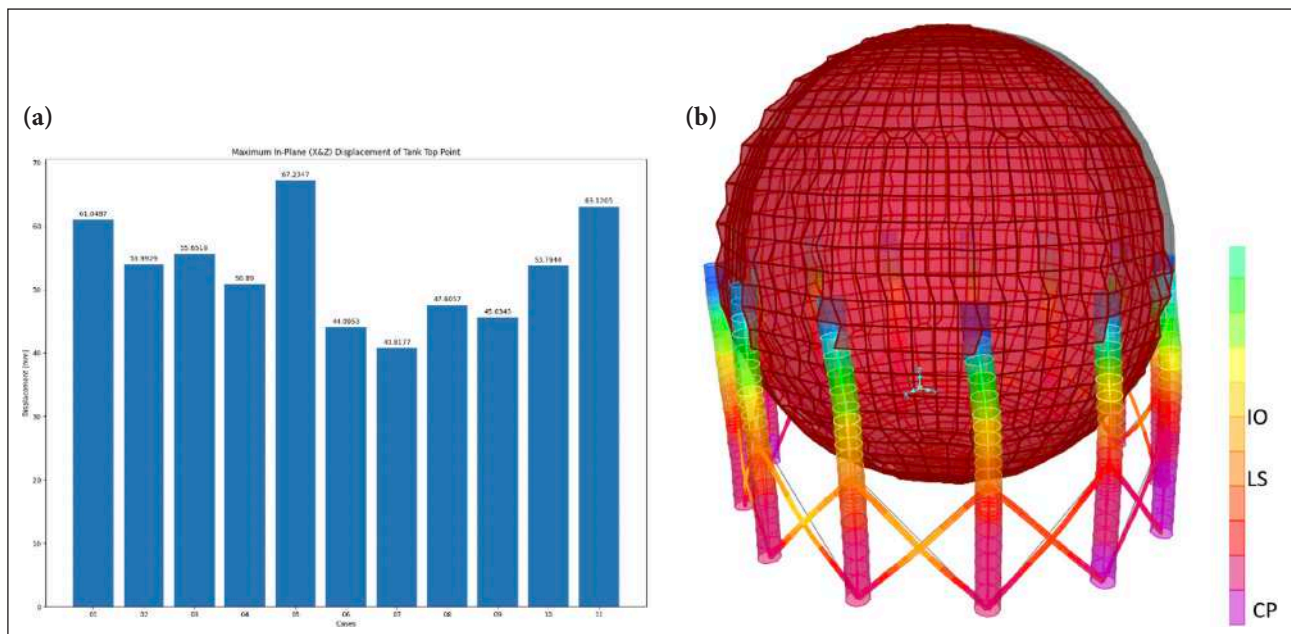


Figure 13. (a) Top displacement values and (b) Deformed shape of LNG Tank*.

*CP stands for Collapse Prevention, LS for Life Safety, and IO for Immediate Occupancy performance levels.

The seismic isolation option is eliminated due to the high displacement demands, which require the replacement of many pipelines. Viscous and Friction damper retrofit solutions, were found rational; however, due to stricter drift values, friction-type dampers (Fig. 14) emerged as the preferable solution.

The primary motivation for selecting friction-type dampers was to enhance the structure's damping and diminish the base shear forces experienced during seismic events. For this case, linear friction dampers have been used.

The retrofitting model is presented in Figure 15.

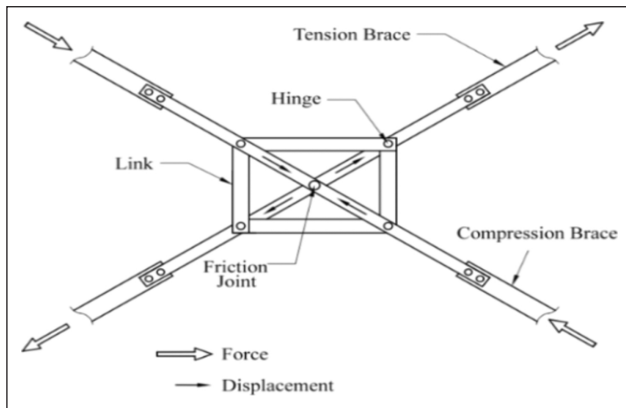


Figure 14. Friction damper type.

Analysis revealed that the current braces were operating beyond their capacity, necessitating their replacement with CHS 219.1/16 pipe profiles in conjunction with the introduction of friction-type dampers. The newly added braces were chosen based on their ability to exceed the axial compression load capacity of the dampers. This retrofitting strategy eliminates the need for further modifications to the existing structure.

Friction dampers featuring varying yield strengths were evaluated to identify the optimal retrofit configuration (Table 5).

Typical base shear and top deformation plots have been provided in Figure 16.

As demonstrated in Table 5, the friction damper with a yield strength of 350kN offers the optimal solution. This is because an increase in yield strength directly increases earthquake demands, thus increasing the base shear and potentially necessitating foundation retrofitting. The hysteresis curve of friction damper with 350kN yield strength and 5 cm target displacement is provided in Figure 17.

Analysis results with friction damper having 350kN yield strength indicate that the average displacement at the top of the columns, relative to the foundation, is 12.41cm, corresponding to 1% of the column height.

Based on the obtained rotation values, capacity evaluations of the columns showed that the Immediate Occupancy limit, as specified by ASCE 41–13 [23], was not exceeded on average. It was noted that columns, which previously partially exceeded their capacities, remained within their

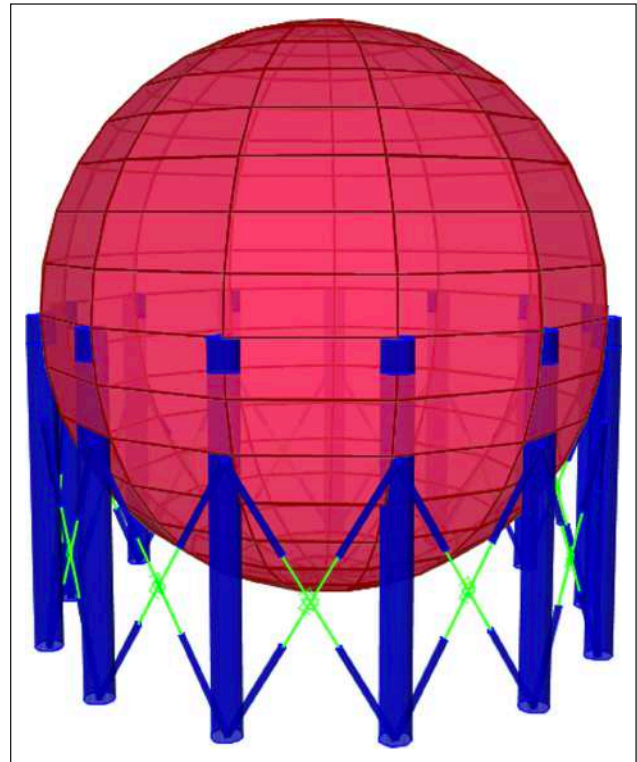


Figure 15. Model of retrofitted LNG tank with friction damper.

capacity values after strengthening. The deformed shape of the retrofitted LNG tank is depicted in Figure 18.

The rotation demands of the steel column for the retrofitted structure decreased by 10% compared to the existing LNG tank. Furthermore, the axial strain demand of braces in the retrofitted LNG tank structure remains within the strain capacity, as shown in Figure 19. Based on the updated FSI analyses, it has been determined that a reduction in the velocity response reduced the inertial and sloshing forces of the included viscous materials by as much as 70%.

3. RESULT AND DISCUSSION

This study focused on the seismic performance assessment and retrofitting of an existing steel LNG Tank near the North Anatolian Fault (NAF) line. The evaluation revealed that the structure's column rotations and the axial deforma-

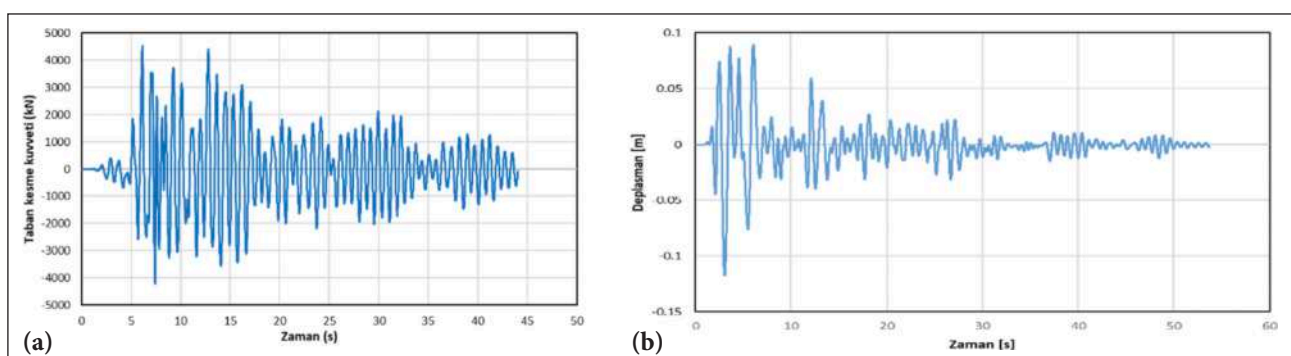


Figure 16. (a) RSN6 record base shear plot and (b) RSN6 record top displacement plot.

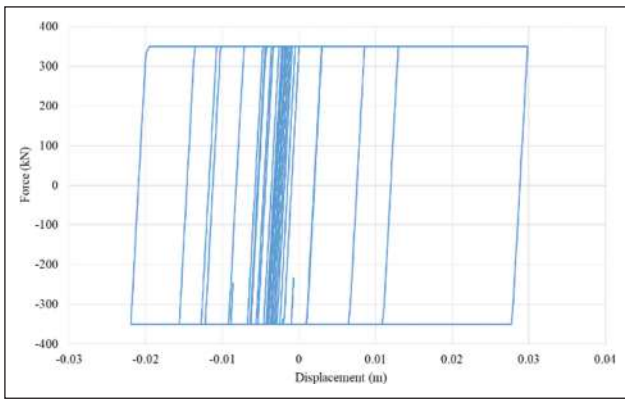


Figure 17. Hysteresis behavior of friction damper (yield strength 350 kN).

tions of the braces did not satisfy the desired seismic performance criteria. Consequently, a retrofitting approach was proposed, incorporating friction dampers alongside new steel braces. The primary aim of introducing additional damping was to minimize operational downtime during the retrofit process and to eliminate the need for foundation retrofitting.

4. CONCLUSION

Implementing friction dampers successfully reduced the inertial, sloshing seismic loads and the total base shear demand on the structure, eliminating the necessity for foundation retrofitting. The total base shear reduction is approximately 68%, the increase in the top displacement is approximately 3%, and the decrease in the column axial forces is approximately 34%. The expected nominal displacement of the link elements is approximately 35 mm. Since the yield force of the links is constant, the member results are not significantly affected by ground motions, including pulse behavior; however, a slight increase in the link and top displacement is observed. This study does not address the long-term effects due to heat, dust, stick-slip, or other maintenance-related factors, which will be that's for future research together with instrumentation of the retrofitted structure to collect data from actual seismic events, enhancing the understanding and validation of retrofitting strategies.

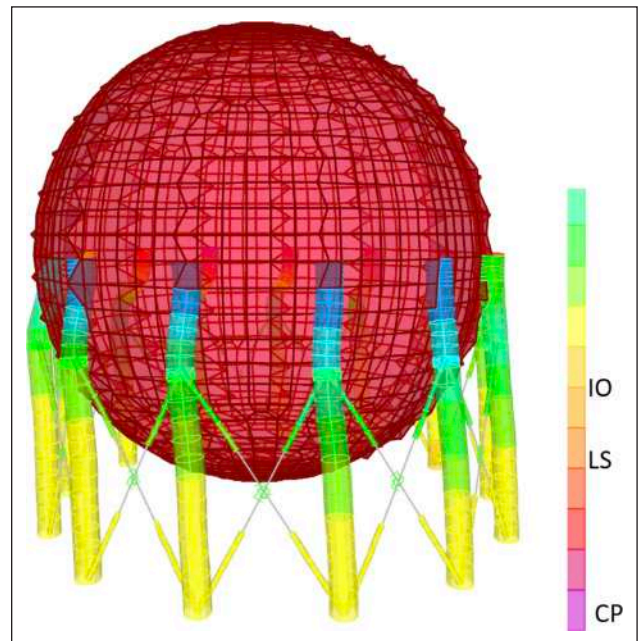


Figure 18. Deformed shape of retrofitted LNG tank.

ETHICS

There are no ethical issues with the publication of this manuscript.

DATA AVAILABILITY STATEMENT

The authors confirm that the data that supports the findings of this study are available within the article. Raw data that support the finding of this study are available from the corresponding author, upon reasonable request.

CONFLICT OF INTEREST

The authors declare that they have no conflict of interest.

FINANCIAL DISCLOSURE

The authors declared that this study has received no financial support.

USE OF AI FOR WRITING ASSISTANCE

Not declared.

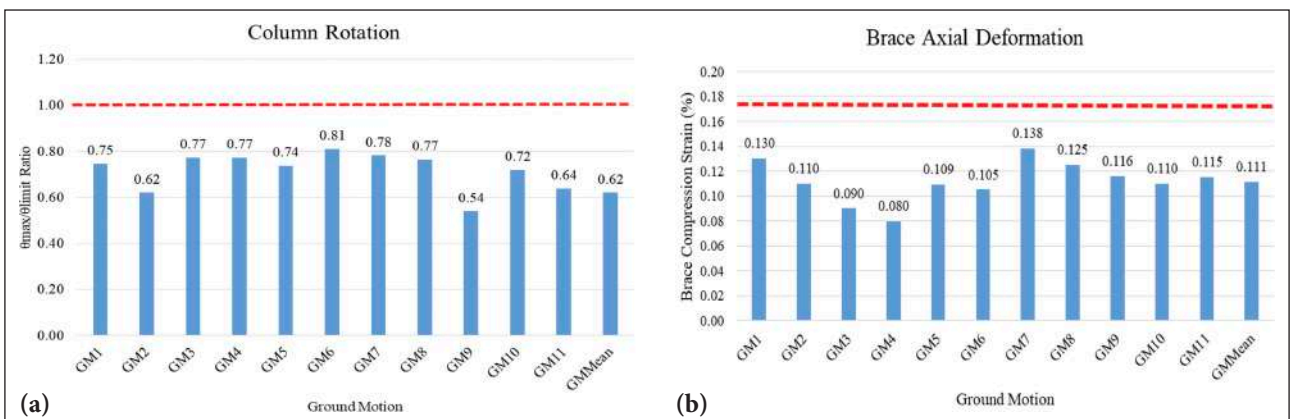


Figure 19. (a) Column rotation and (b) Steel brace axial compression strain for retrofitted LNG tank.

*CP stands for Collapse Prevention, LS for Life Safety, and IO for Immediate Occupancy performance levels.

PEER-REVIEW

Externally peer-reviewed.

REFERENCES

- [1] Shekari, M. R., Khaji, N., & Ahmadi, M. T. (2010). On the seismic behavior of cylindrical base-isolated liquid storage tanks excited by long-period ground motions. *Soil Dyn Earthq Eng*, 30, 968–980. [\[CrossRef\]](#)
- [2] Niwa, A., & Clough, R. W. (1982). Buckling of cylindrical liquid-storage tanks under earthquake loading. *Earthq Engng Struct Dyn*, 10, 107–122. [\[CrossRef\]](#)
- [3] Shaban, N., Ozdemir, S., Caner, A., & Akyüz, U. (2017, June 15-17). *Seismic retrofit of buildings with backbone dampers*. In Proceedings of the ECCOMAS Thematic Conference—COMPDYN 2017: 6th International Conference on Computational Methods in Structural Dynamics and Earthquake Engineering: An IACM Special Interest Conference, Programme, Rhodes Island, Greece. [\[CrossRef\]](#)
- [4] Gregoriou, V. P., Tsinopoulos, S. V., & Karabalis, D. L. (2011, May 25-28). *Dynamic analysis of liquefied natural gas tanks seismically protected with energy dissipating base isolation systems*. In Proceedings of the ECCOMAS Thematic Conference—COMPDYN 2011: 3rd International Conference on Computational Methods in Structural Dynamics and Earthquake Engineering: An IACM Special Interest Conference, Programme, Corfu, Greece.
- [5] Jadhav, M. B., & Jangid, R. S. (2006). Response of base-isolated liquid storage tanks to near-fault motions. *Struct Eng Mech*, 23, 615–634. [\[CrossRef\]](#)
- [6] Ozbulut, O. E., Bitaraf, M., & Hurlebaus, S. (2011). Adaptive control of base-isolated structures against near-field earthquakes using variable friction dampers. *Eng Struct*, 33, 3143–3154. [\[CrossRef\]](#)
- [7] Saha, S. K., Matsagar, V. A., & Jain, A. K. (2014). Earthquake response of base-isolated liquid storage tanks for different isolator models. *J Earthq Tsunami*, 8, 1450013. [\[CrossRef\]](#)
- [8] Çerçevik, A. E., Avsar, Ö., & Hasançebi, O. (2020). Optimum design of seismic isolation systems using metaheuristic search methods. *Soil Dyn Earthq Eng*, 131, 106012. [\[CrossRef\]](#)
- [9] Çalım, F., Güllü, A., Soydan, C., & Yüksel, E. (2023). State-of-the-art review for lead extrusion dampers: Development, improvement, characteristics, application areas, and research needs. *Structures*, 58, 105477. [\[CrossRef\]](#)
- [10] Güllü, A., Smyrou, E., Khajehdehi, A., Ozkaynak, H., Bal, I. E., Yüksel, E., & Karadogan, F. (2019). Numerical modeling of energy dissipative steel cushions. *Int J Steel Struct*, 19, 1331–1341. [\[CrossRef\]](#)
- [11] Balazic, J., Guruswamy, G., Elliot, J., Pall, R. T., & Pall, A. (2011). *Seismic rehabilitation of justice headquarters building*. 12th WCEE 2000.
- [12] Soli, B., Baerwald, D., Krebs, P., & Pall, R. T. (2004, August 1-6). *Friction Dampers for Seismic Control of Ambulatory Care Center, Sharp Memorial Hospital, San Diego, CA*. 13th World Conference on earthquake Engineering, Paper No. 1953.
- [13] Housner GW. (1957). Dynamic pressure on accelerated fluid containers. *Bull Seismol Soc Am*, 47(1):15–35. [\[CrossRef\]](#)
- [14] Haroun, M.A., & Housner, G.W. (1981). Earthquake response of deformable liquid storage tanks. *J Appl Mech*, 48, 411–418. [\[CrossRef\]](#)
- [15] Erdik, M., Demircioglu, M., Sesetyan, K., Durukal, E., & Siyahi, B. (2004). Earthquake hazard in Marmara Region, Turkey. *Soil Dyn Earthq Eng*, 24(8), 605–631. [\[CrossRef\]](#)
- [16] Giardini, D., Woessner J., & Danciu L. (2014). SHARE Project: Mapping Europe's Seismic Hazard. *EOS*, 95(29): 261–262. [\[CrossRef\]](#)
- [17] Caltrans. (2013). *Caltrans seismic design criteria, version 1.7*. California Department of Transportation.
- [18] ASCE. (2010). *Minimum design loads for buildings and other structures*. ASCE Standart, ASCE 7- 10.
- [19] Turkish Building Earthquake Code. (2018). *Specification for buildings to be built in seismic areas*. Ministry of Public Works and Housing, Ankara, Türkiye.
- [20] Hasanoğlu, S., Güllü, A., Dindar, A. A., Müderisoğlu, Z., Özkaynak, H., & Bozer, A. (2024). Optimal selection and scaling of ground motion records compatible with input energy and acceleration spectra. *Earthq Eng Struct Dyn*, 53(7), 2382–2404. [\[CrossRef\]](#)
- [21] Güllü, A. (2023). A compendious review on the determination of fundamental site period: Methods and importance. *Geotechnics*, 3(4), 1309–1323. [\[CrossRef\]](#)
- [22] Güllü, A., Hasanoğlu, S., & Yüksel, E. (2022). A practical methodology to estimate site fundamental periods based on the KiK-net Borehole Velocity Profiles and its application to Istanbul. *Bullet Seismol Soc Am*, 112(5), 2606–2620. [\[CrossRef\]](#)
- [23] ASCE. (2013). *Seismic Evaluation and Retrofit of Existing Buildings*. ASCE 41-13.